An Investigation of the Acceleration Induced Burning Rate Increase of Nonmetallized Composite Propellants

E. J. STURM* AND R. E. REICHENBACH†
Naval Postgraduate School, Monterey, Calif.

A model is developed which correlates the experimentally observed burning rates of composite nonmetallized propellants subjected to acceleration fields normal to the burning surface. The model attributes the increased burning rates to additional energy transfer to the propellant surface from the combustion of ammonium perchlorate particles retained on the propellant surface by the acceleration forces. A method for predicting, with limited experimental data, the burning rate of a propellant as a function of pressure and acceleration is described.

Nomenclature

a = acceleration
a_o = standard acceleration of gravity
b_1, b_2 = constants
d_p = diameter of AP particle
d_{pc} = diameter of an AP particle of critical size
f = fraction of energy release transferred to the propellant surface
F_b = body force
F_d = drag force
G = acceleration in gravitational units a/a_o
h_c = energy released by the decomposition and combustion of AP
h_v = energy required to gasify a unit mass of propellant
J = fraction of additional small sized AP mass which decomposes on the propellant surface due to the acceleration induced AP body force increase, $0 \leq J \leq 1$
K_1 = constant
M = molecular weight
p = pressure
r = burning rate with acceleration
r_o = burning rate without acceleration
R = universal gas constant
T_g = mean temperature of the gas phase
T_o = initial propellant temperature
V_g = mean velocity of the combustion products away from the propellant surface
V_p = oxidizer particle velocity
W_o = weight percent small AP (smallest cut) in the propellant formulation
$\Delta\dot{Q}$ = additional heat-transfer rate to the propellant surface defined by Eq. 8
η = $W_o h_c/h_v$
μ_g = viscosity of the propellant gas phase
ρ_g = mean density of the gas phase
ρ_p = density of an AP particle
ρ_s = density of the solid propellant phase

Introduction

SOLID-PROPELLANT rocket motors are being used for applications that subject their propellant grains to large radial acceleration fields. The burning rate of nonmetallized propellants increases significantly when the induced acceleration field is greater than 100 G and is normal and into the propellant burning surface.[1,2]

Experimental and theoretical studies have been performed to determine the effects of the various propellant parameters on the burning rate increase. Based on the experimental results, some burning rate behavioral trends have been established.[1,2] Glick[3] has performed a theoretical analysis of the acceleration induced burning rate augmentation for nonmetallized propellants using a model which is an extension of Summerfield's granular diffusion flame model (GDFM).[4] Some important experimental results[1,2,5] are not adequately correlated by Glick's model.

An analysis is presented which correlates the data obtained during a recent experimental investigation.[2] Based on the analysis, a method is developed which enables the burning rate for a given propellant to be predicted as a function of pressure and acceleration with limited experimental data.

Model

The model developed in this paper is an extension of Fenn's phalanx flame model[6] for the combustion of nonmetallized composite solid propellants burning under standard acceleration conditions. Fenn represents the flame (Fig. 1) as burning in a gaseous reaction zone centered at the interface of streams of fuel and oxidizer which are generated by the vaporization of each solid component. The reaction zone is assumed to be comprised of two distinct regions, a premixed combustion region located at the base of a diffusion controlled region. The relative size of the two distinct regions depends on the pressure. At low pressures, where the rate of diffusion is greater than the rate of chemical reaction, the reaction zone is entirely a premixed combustion flame. At high pressures, where the chemical reaction rates are fast compared to the diffusion rates, the reaction zone is primarily a diffusion controlled flame. However, Fenn postulates that even at very high pressures, there exists a microscopically small premixed region at the base of the reaction zone.

The reaction zone is a "phalanx" which spearheads the attack of the hot reaction gases on the unburned solid. The vicinity of the interface between the two solid phases receives the greatest heat flux from the reaction zone, and solid component vaporization occurs most rapidly near the interface. Fenn assumes that it is the rate at which this phalanx reaction zone proceeds into the propellant that is characteristic of the propellant burning rate.

Received March 3, 1969; revision received October 6, 1969. This work was supported by Naval Ordnance Systems Command, Request 17-7-5073.

* Lieutenant Commander, U.S. Navy; now with the Naval Air Systems Command, Washington, D.C.

† Associate Professor; now Research Staff Member, Science and Technology Division, Institute for Defense Analyses, Arlington, Va.

Fenn's analysis yields the following burning rate vs pressure dependence:

$$r_o = p/(b_1 + b_2 r_o p^{1/3}) \quad (1)$$

According to Fenn's model the flame phalanx follows its penetration course along the interface between the fuel and oxidizer. The phalanx flame may proceed completely around the oxidizer particle before the particle is entirely consumed. The oxidizer particle would then become separated from the fuel matrix by a thin gas film. If the pressure suddenly dropped, as in extinguishment experiments, the oxidizer particles would be "blown out" of their cavities by the expanding gas layer leaving a "bore-hole" in the fuel matrix. Such bore-holes have been found in extinguished burning surfaces.[7]

The drag forces produced by the normal gas flow from the gasifying surface could deplete the propellant surface of small oxidizer particles. At high pressures the increased phalanx flame penetration rate could result in an increase in the depletion of oxidizer at the propellant surface causing a plateau or drop in the burning rate-pressure curve or even "pressure extinguishment." Both of these phenomena have been observed, especially with small-size oxidizer particles in fuel rich propellant compositions.[7]

The possibility posed by Fenn that a phalanx flame may burn completely around an oxidizer particle in the vicinity of the oxidizer particle-fuel matrix interface prior to the complete combustion of the oxidizer particle can thus explain certain experimental evidence that Summerfields's GDFM (a one-dimensional model) can not explain. This same possibility leads to a consideration of the retention of the decomposing oxidizer particles on the propellant surface by centrifugal or body forces and forms the basis of the analysis presented in this paper.

The assumptions incorporated in the following analysis, which is based on an idea similar to that proposed by Crow and Willoughby for the acceleration induced burning rate augmentation of metallized propellants,[5] can be summarized as follows: 1) the acceleration augmented burning rate of nonmetallized propellants is steady in the mean;‡ 2) small ammonium perchlorate (AP) oxidizer particles evolved at the burning surface become separated from the fuel matrix by a thin gas layer when the phalanx flame is able to burn completely around the AP particle-fuel matrix interface before the AP particle is consumed; 3) an AP oxidizer particle will remain on the surface until it has decomposed to a size such that the aerodynamic drag forces remove it from the surface; and 4) the burning rate increase in an acceleration field is proportional to the amount of additional energy that is transferred to the propellant surface from the exothermic decomposition of these AP particles and the subsequent reaction of oxidizer rich AP decomposition products with the fuel vapor from the pyrolyzed fuel matrix.

The assumption that only the small AP particles become separated from the fuel matrix by a thin gas layer was made because the phenomena of bore-holes, plateaus, and pressure extinguishment occur with propellants that generally contain small-size oxidizer particles.

An acceleration force field into the burning surface will impede the motion of the oxidizer particles away from the surface. The body force, F_b, on an assumed spherical particle is

$$F_b = \pi d_p^3 \rho_p a/6 \quad (2)$$

Assuming Stokes flow, the drag force F_d on a spherical oxidizer particle is given by

$$F_d = 3\pi \mu_g d_p (V_g - V_p) \quad (3)$$

where V_g is the gas phase velocity equal to $r\rho_s/\rho_g$ (cm/sec).

‡ This assumption was verified experimentally for nonmetallized propellants.[2] As shown in Ref. 2 this is not a valid assumption for metallized propellants.

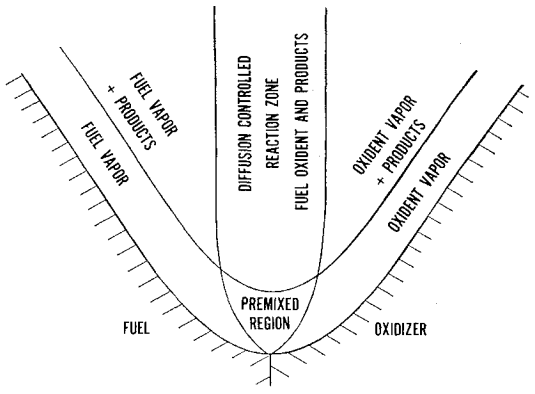

Fig. 1 Phalanx flame at steady state (after Fenn[6]).

The equality

$$F_b = F_d \quad (4)$$

represents the condition in which the centrifugal forces balance the aerodynamic forces, and a particular size oxidizer particle, with a diameter defined as the critical diameter, remains on the surface. At a given acceleration, all those particles which have a diameter larger than the critcial diameter, d_{pc}, will be retained on the surface, while those particles which have a diameter smaller than the critical diameter will escape the surface. Setting $V_p = 0$ and substituting Eqs. (2) and (3) into Eq. (4) and solving for d_{pc} yields

$$d_{pc} = 6(\mu_g r \rho_s / 2\rho_g \rho_p a)^{1/2} \quad (5)$$

The magnitude of the critical diameter can easily be estimated as a function of acceleration by substituting representative values of the parameters in Eq. (5). The following representative values were used: $\mu_g = 4 \times 10^{-4}$ g/cm/sec, $r = 0.765$ cm/sec, $\rho_s = 1.65$ g/cm^3, $\rho_p = 1.95$ g/cm^3, $T_g = 1775$°K, $M = 22$ g/g-mole. Assuming a perfect gas, the following relations for pressures of 500 and 1000 psia were obtained:

$$d_{pc_{500}} = 304[1/G]^{1/2} \text{ (microns)} \quad (6)$$

$$d_{pc_{1000}} = 216[1/G]^{1/2} \text{ (microns)} \quad (7)$$

These equations indicate that the critical particle sizes for acceleration levels above 100 G are of the same order of magnitude as small-size oxidizer particles used in typical multimodal propellants.

Solid AP oxidizer particles exothermally decompose, forming oxidizer rich products which subsequently burn with the fuel gases released by the pyrolysis of the fuel binder. The retention of AP oxidizer particles on the surface of the propellant increases the amount of oxidizer rich decomposition products available at the surface of the propellant. This in turn increases the amount of fuel which is combusted near the propellant surface. This results in increased heat transfer to the surface and hence, an increased burning rate. This additional heat transfer to the surface and the resulting increase in burning rate can be expressed as

$$\Delta \dot{Q} = \rho_s r W_o h_c f J = \rho_s (r - r_o) h_v \quad (8)$$

Solving Eq. (8) for the burning rate ratio, it is found that

$$r/r_o = [1 - (W_o f h_c J/h_v)]^{-1} \quad (9)$$

Examination of Eq. (9) indicates that the larger the term $W_o f h_c J/h_v$, the larger the burning rate ratio will become. It is apparent that the terms in the factor $W_o h_c/h_v$ ($\equiv \eta$) are primarily a function of the particular propellant. If for two different propellants the values of f and J are equal, the propellant with the largest value of η will exhibit the greatest sensitivity to acceleration.

The parameter f represents the fraction of the energy release (by the decomposition of the AP particles and subse-

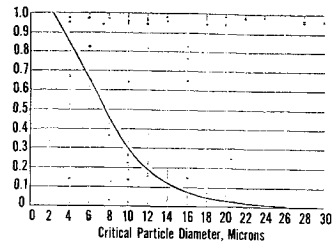

Fig. 2 Values of J vs critical particle diameter.

quent combustion of the AP decomposition products and fuel vapor) that is transferred to the propellant surface. The value of f will depend on the temperature gradient in the gas phase above the propellant surface. The theories of both Summerfield and Fenn predict that at pressures of interest in rocket motor applications (where diffusion is the rate controlling phenomenon) increasing the pressure will move the combustion zone closer to the propellant surface at a rate proportional to the one-third power of the pressure [Eq. (1)]. Thus f should increase at a rate proportional to the one-third power of pressure. Referring again to Eq. (9), it is seen that increasing f by increasing the pressure while holding η and J constant will increase the burning rate ratio. That is, higher pressure will lead to greater acceleration sensitivity.

Once steady-state burning has been achieved, the parameter J will depend on the small AP oxidizer particle size distribution, pressure, propellant burning rate, acceleration level, and the amount of AP particle mass consumed before the phalanx flame separates it from the propellant surface. The fraction J will be proportional to the additional mass consumed in all those small AP particles larger than critical size as they decompose to critical size. Thus, for a given critical particle diameter, the value of J will depend on the particle size distribution; if the particle size distribution is such that a very small percentage of the particles are larger than the critical particle diameter, the value of J will be small. In contrast, if the particle size distribution is such that most of the particles are larger than the same given critical particle diameter, the value of J will be relatively large. Increasing J will increase the burning rate ratio of a given propellant if f (i.e., pressure) is held constant.

Equation (9) can be used to predict the burning rate behavior of a particular propellant if values of W_o, h_c, h_v, f, and J are known. The terms W_o, h_c, h_v are functions of a particular propellant and, with the exception of W_o, can only be determined approximately prior to experimentation. The term f is a function of pressure which appears to have to be determined by using experimental data. The shape of the burning rate ratio vs acceleration curve for a particular propellant is controlled by the dependence of the parameter J on acceleration level. A method that can be used to obtain this dependence follows.

Using Eq. (5) and the perfect gas law, it is easily shown that

$$d_{p_c} = K_1[r/Gp]^{1/2} \text{ (microns)} \tag{10}$$

where

$$K_1 = 6 \times 1.9 \times 10^3 \left[\frac{\mu_g \rho_s R T_g}{2\rho_p a_o \bar{M}}\right]^{1/2} \text{microns}\left(\frac{\text{lbf/sec}}{\text{in.}^3}\right)^{1/2} \tag{11}$$

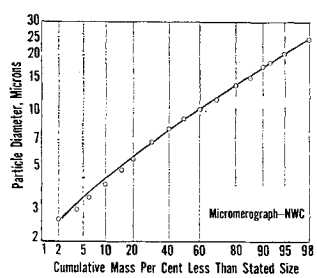

Fig. 3 Ammonium perchlorate size distribution.

The factor 1.9×10^3 is the conversion factor which allows substitution of r in units of in./sec and p in units of lbf/in.^{2} to yield d_{p_c} in units of microns.

The assumption that K_1 is a constant is equivalent to assuming that μ_g and T_g do not vary with acceleration. Since the critical particle diameter is a function of Gp/r, a prediction of J vs Gp/r can be made in the following manner. Given a value of Gp/r, the critical particle diameter (d_{p_c}) can be calculated using Eq. (10) and an estimate for K_1. This value of d_{p_c} and the distribution of small-size AP can then be used to evaluate J (see Appendix). Figure 2 (J vs d_{p_c}) was obtained for the distribution of small AP particles shown in Fig. 3. Thus, the acceleration dependence of J can be ascertained if K_1 and the small-size AP distribution are known. The latter can be assumed to be known, whereas the former can only be determined approximately prior to experiment.

In summary, the theory predicts that: 1) no burning rate augmentation will occur until reaching a threshold acceleration sufficient to hold on the propellant surface AP particles that would otherwise escape the surface; 2) the burning rate will increase with acceleration as more of the AP particle mass is consumed on the propellant surface; 3) a limit burning rate is achieved at high acceleration levels when all the AP particle mass is consumed on the propellant surface; 4) increasing the pressure will result in larger values of burning rate ratio for a given propellant; 5) increasing the weight percentage of the fine oxidizer particles in otherwise similar propellants will result in larger values of burning rate ratio; and 6) increasing the basic burning rate of a propellant will decrease the effect of acceleration on the burning rate of a propellant. The last two observations are somewhat interrelated since increasing the weight percentage of the fine AP particles generally results in a faster basic burning rate. The net effect on the acceleration sensitivity obtained by increasing the weight percentage of the fine AP particles would depend on how much the increased basic burning rate offsets the detrimental effect of increasing the weight percentage of the fine AP particles. If burning rate catalysts are used to increase the basic burning rate of the propellant and no change is made in the weight percentage of the fine AP particles, the theory predicts without reservation that the acceleration sensitivity of the propellant will be reduced (by increasing d_{p_c} for a given acceleration level and pressure).

Comparison of Theory with Experiment

The theory is compared with experimental results obtained during the course of a research program conducted at the Naval Postgraduate School. The experiments were conducted with a centrifuge using conventional strand burning techniques. The average burning rates of three nonmetallized propellants were determined in acceleration fields up to 1000 G at pressures of 500 and 1000 psia. The acceleration field was directed normal and into the propellant burning surface. Detailed information concerning the experimental equipment and procedures is contained in Refs. 1 and 2.

The propellant formulations prepared by the Naval Weapons Center (NWC), contained spherical AP oxidizer and PBAN binder. The weight ratio of AP to PBAN in every formulation was constant at 79 parts AP to 21 parts PBAN. The AP size distributions were made as narrow as possible to study the effect of oxidizer particle size on burning rate aug-

Table 1 Nonmetallized propellant data

Propellant designator	500 psia		1000 psia	
	r/r_o max	ηf	r/r_o max	ηf
P410	1.230	0.187	1.285	0.222
P411	1.435	0.303	1.630	0.387
P420	1.286	0.222	1.440	0.306

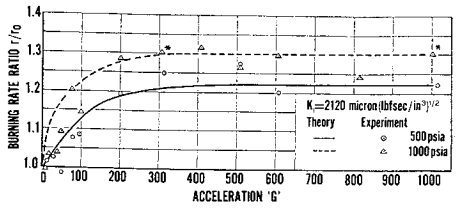

Fig. 4 Comparison of theory with experiment for P410 propellant.

mentation. All propellants contained bimodal AP distributions. The specific formulations were as follows:

P410: 19.62% 9μAP, 59.38% 94μAP, 21% PBAN
P411: 34.00% 9μAP, 45.00% 94μAP, 21% PBAN
P420: 19.62% 9μAP, 59.38% 200μAP, 21% PBAN

A summary of the experimental results for the three propellants is shown in Figs. 4–6.

It is reasonable to assume that the value of J approached unity at acceleration levels greater than 600 G because the data indicate that the burning rate ratio approached a constant value for a given pressure and propellant at these high acceleration levels. Values of ηf, shown in Table 1, were obtained by using Eq. (9) with $J = 1$ and r/r_o equal to the high acceleration (> 600 G) limit burning rate ratio as shown in Figs. 4–6.

Since the the three propellants contain the same oxidizer and the same binder, the value of h_c should be the same for all three propellants. Furthermore, since the propellants all contain 79% AP and 21% PBAN, they should have approximately equal values of h_v. Therefore, the individual propellant values of η ($= W_o h_c/h_v$) should vary directly as the weight percentage of the small size AP oxidizer particles, W_o. Since the value of f depends on pressure and not the particular propellant, it follows from the previous considerations that values of ηf at a given pressure should be in the same ratio as the values of W_o for the three propellants. A comparison of the ratios of W_o and the ratios of the calculated ηf is shown in Table 2. The agreement between P410 and P411 propellants is excellent; between P420 and the two P410 series propellants only fair. However, the experimentally determined ηf ratios all trend in the correct manner. Thus, it is believed that Eq. (9), through the parameter W_o, is able to predict the relative acceleration sensitivities of a series of propellants that have different values of W_o. The values of ηf for a given propellant should increase with increasing pressure because of the factor f. The ratio of

$$(\eta f)_{1000 \text{ psia}}/(\eta f)_{500 \text{ psia}} \tag{12}$$

for a given propellant should be $(1000)^{1/3}/(500)^{1/3} = 1.26$ since f should vary as the one-third power of pressure and η is invariant with pressure. The experimentally determined f ratios were: P410, 1.189; P411, 1.178; and P420, 1.378. Thus Eq. (9) is able to predict reasonably well the pressure dependence of propellants P410, P411, and P420 at high acceleration levels.

The ability of the analysis to predict the acceleration dependence of the burning rate ratio can be determined by constructing burning rate ratio vs acceleration curves for the three propellants and then comparing the predicted dependence with the experimental results. This was done for all three propellants at both pressure levels. The theoretical curves were constructed using a method which can be used to

Table 2 Propellant comparison

Propellant comparison	W_o ratio	500 psia ηf ratio	1000 psia ηf ratio
P410/P411	0.577	0.617	0.574
P410/P420	1.000	0.843	0.725
P411/P420	1.731	1.365	1.265

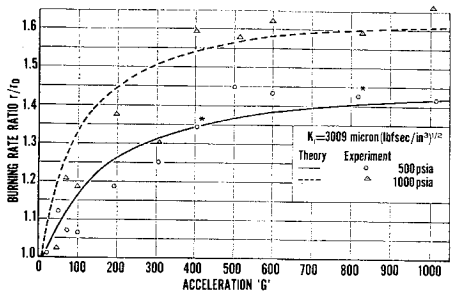

Fig. 5 Comparison of theory with experiment for P411 propellant.

obtain the pressure and acceleration dependence of the burning rate for any propellant. A detailed description of the construction of the curves in Fig. 5 for propellant P411 will serve to present the method and demonstrate its use. To construct the curves in Fig. 5, it was assumed that the burning rate of P411 had been determined at 500 psia and three acceleration levels, 1 G, 403 G, and 811 G (the data points marked with an asterisk in Fig. 5). The burning rates at 811 G (0.379 in./sec) and 1 G (0.265 in./sec) were used to determine the limit burning rate ratio (1.430) at 811 G. This limit burning rate ratio value was substituted into Eq. (9) with $J = 1$, to obtain a value of $W_o h_c f/h_v$ equal to 0.301. The experimental burning rate ratio obtained at the intermediate G level ($r/r_o = 1.344$) was then used to solve for the corresponding value of J using the value of $W_o h_c f/h_v$. Thus $J = 0.850$ and $Gp/r = 5.66 \times 10^5$ at 403 G were obtained for propellant P411. The plot of Fig. 2 yielded a value d_{pc} equal to 4.0 μ for this value of J with the known particle size distribution (used in constructing Fig. 2). Then using the values d_{pc} and Gp/r and Eq. (10), the constant K_1 was evaluated as 3009 μ (lbfsec/in.^{3})$^{1/2}$.

The burning rate ratio vs acceleration curve for the propellant was then constructed in the following manner. Representative values of Gp/r were chosen and the corresponding values of d_{pc} were determined using Eq. (10). Then Fig. 2 yielded values of J. These values of J were substituted into Eq. (9) (with the value of $W_o f h_c/h_v$ determined from the high acceleration level experiment) to obtain values of r/r_o. The variation of r/r_o with Gp/r was then known. Since the pressure was known, it was then possible to calculate the values of r/r_o vs G. The curve for propellant P411 at 500 psia shown in Fig. 5 was constructed in this manner.

The pressure dependence for this propellant was determined through the parameter f. Using the value of $W_o f h_c/h_v$ obtained from the experiment done at the high acceleration level at the original pressure level, a new value of $W_o f h_c/h_v$ for the desired new pressure level was calculated from the expression

$$\frac{W_o f h_c/h_v|\text{pressure 1}}{W_o f h_c/h_v|\text{pressure 2}} = \left[\frac{(\text{pressure 1})}{(\text{pressure 2})}\right]^{1/3} \tag{13}$$

A series of values of Gp/r were chosen and the corresponding values of d_{pc} were obtained using the value of K_1 determined

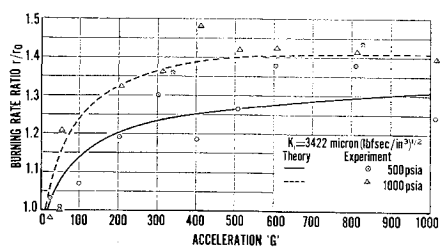

Fig. 6 Comparison of theory with experiment for P420 propellant.

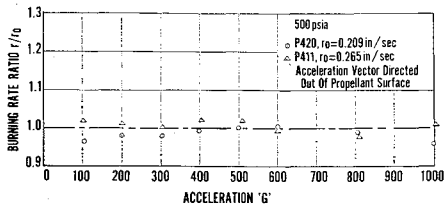

Fig. 7 Burning rate ratio vs acceleration with acceleration vector directed out of propellant surface.

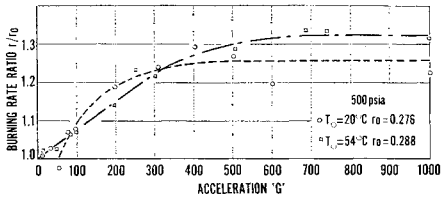

Fig. 8 Burning rate ratio vs acceleration as a function of initial propellant temperature for propellant P410.

at the original pressure level. The method outlined above was used to obtain the values of r/r_o vs G (see the curve for 1000 psia in Fig. 5). The pressure dependence through the parameter f should be valid over the pressure range for which the combustion zone thickness is diffusion rate controlled and hence proportional to the one-third power of the pressure.

Theoretical curves for the other two propellants were constructed at both pressure levels and are presented in Figs. 4 and 6. The data points marked with asterisks and the one G burning rates are the experimental data that were assumed known and from which the theoretical curves were constructed. The other data points are shown in the figures to allow comparison of the experimental data with the theoretical curves. As can be seen from Figs. 4–6, the theory is able to predict reasonably well the acceleration and pressure dependence of burning rate ratio for all three propellants. The values of K_1 used to construct the theoretical curves are about one-quarter the value of 12380 μ (lbfsec/in.^{3})$^{1/2}$ obtained if the aforementioned typical values of the thermophysical properties are substituted into Eq. (11) which assumed Stokes drag law. Stokes drag law is valid for spheres with no mass flux from the surface at low Reynolds number (Re <1). The small AP oxidizer particles are not true spheres and have a mass flux out of their surface since they are decomposing. It is known that the drag on a burning particle[8] is as much as an order of magnitude less than that predicted by Stokes drag law for the low-Reynolds number range (<10) encountered in small particle-low gas velocity conditions. Since the numerator of K_1 is proportional to the square root of the particle drag, it follows that the value of K_1 for a decomposing particle would be a factor of $(10)^{1/2}$ smaller than the value of K_1 for an inert particle which obeys Stokes drag law. Thus the theory is able to correlate the experiment results with reasonable values of K_1.

When the acceleration is directed out of the propellant burning surface the value of J should be zero. Equation (9) indicates that the propellant burning rate will not be altered in this acceleration condition. The experimental results obtained for P411 and P420 shown in Fig. 7 support this conclusion.

Finally, the theory is able to predict the correct qualitative behavior of the limit burning rate ratio when the initial temperature of the propellant is increased. An examination of the factors in Eq. (9) suggests that the only parameter affected by the propellant initial temperature will be h_v. The higher the initial propellant temperature the lower will be the energy required to heat and gasify a unit mass of propellant (h_v). Thus, for a given propellant (W_o and h_c const), at a constant pressure (f const) and the high-acceleration limit ($J = 1$), the effect of increasing the initial propellant temperature (and hence decreasing h_v) will be to increase r/r_o. This agrees with the experimental results obtained for propellant P410, which are shown in Fig. 8.

Conclusions

An analytical model that attributes the increase in propellant burning rate in acceleration field to the retention of the fine AP oxidizer particles on the propellant surface was developed. The model was successfully employed to correlate the results obtained during the course of an experimental study of acceleration induced burning rate augmentation. The model suggests that the acceleration effects can be minimized by decreasing the weight percentage of the fine AP particles in multimodal propellants and increasing the basic burning rate of the propellant by the use of burning rate catalysts.

Appendix

Particle size distributions as shown in Fig. 3 are described in terms of cumulative mass percentage. The mass fraction, J, of the 9 μ mass mean diameter (mmd) AP distribution removed by decomposition at the propellant surface as a function of critical particle diameter, d_{pc}, was estimated in the following manner. It was assumed that none of the small AP particle mass had burned before the phalanx flame separated it from the propellant surface. Although this is probably not the case, the assumption is considered in keeping with the approximate nature of the model. The inaccuracy introduced is compensated for by the constant K_1, which must be experimentally determined. The particles in the distribution were considered to be separated according to diameter into 15 increments, each 2 μ wide. The percentage of the entire distribution's mass contained in those particles in each 2 μ increment was obtained from the distribution curve shown in Fig. 3. For example, Fig. 3 shows that 3% of the distribution's mass is contained in particles between 18 and 20 μ in diameter, whereas 8% of the distribution's mass is contained in particles between 12 and 14 μ in diameter.

The assumption was made that the particles were homogeneous and spherical. Then for a given critical particle diameter that fraction of mass removed from a given 2 μ particle size increment was estimated by the equation

$$m_f = 1 - (d_{pc}/d_{pi})^3,\ d_{pi} > d_{pc},\ m_f = 0,\ d_{pi} \leqslant d_{pc}$$

where m_f = fraction of mass removed from a given 2 μ particle size increment; d_{pi} = initial mean particle diameter within a given size increment (assumed equal to the arithmetic mean of the end points of the size increment) (micron).

For a given 2 μ increment, multiplying m_f by the percentage of the particle distribution mass contained within that increment yields the fraction of the original particle mass which is removed from the distribution by reducing all particles in that increment to the given critical diameter. A summation of all the 2 μ size increments yields the fraction of the distribution's mass removed when all the particles in the distribution are reduced to a given critical size.

References

[1] Anderson, J. B. and Reichenbach, R. E., "An Investigation of the Effect of Acceleration on the Burning Rate of Composite Propellants," *AIAA Journal*, Vol. 6, No. 2, Feb. 1968, pp. 271–277.

[2] Sturm, E. J., "A Study of the Burning Rates of Composite Solid Propellants in Acceleration Fields," Ph.D. thesis, AD-832206, March 1968, Naval Postgraduate School, Monterey, Calif.

[3] Glick, R. L., "An Analytical Study of the Effects of Radial Acceleration Upon the Combustion Mechanism of Solid Propellant," Thiokol Rep. 42–66, NASA Rep. 66218, Dec. 1966, Thiokol Chemical Corp., Huntsville, Ala.

[4] Summerfield, M. et al., "Burning Mechanism of Ammonium

Perchlorate Propellants," *ARS Progress in Astronautics and Rocketry: Solid Propellant Rocket Research*, Vol. 1, edited by M. Summerfield, Academic Press, New York, 1960, pp. 142–182.

[5] "Investigation of Particle Growth and Ballistic Effects on Solid Propellant Rockets," UTC 2128-FR, June 1966, BuWeps Contract NOw 65-022f, United Technology Center, Sunnyvale, Calif.

[6] Fenn, J. B., "A Phalanx Flame Model for the Combustion of Composite Solid Propellants," *Combustion and Flame*, Vol. 12, No. 3, Jan. 1968, pp. 201–216.

[7] Bastress, E. K., "Modification of the Burning Rates of Ammonium Perchlorate Solid Propellants by Particle Size Control," Aeronautical Engineering Report 536, ONR Contract Nonr 1858 (32)-NR 098-201, March 1961, Dept. of Aeronautical Engineering, Princeton Univ., Princeton, N.J.

[8] Eisenklam, P., Arunachalam, S. A., and Weston, J. A., "Evaporation Rates and Drag Resistance of Burning Drops," *Eleventh Symposium (International) on Combustion*, The Combustion Institute, 1967, pp. 715–128.

JUNE 1970 AIAA JOURNAL VOL. 8, NO. 6

Use of Ion Probes in Supersonic Plasma Flow

W. E. SCHARFMAN* AND W. C. TAYLOR†
Stanford Research Institute, Menlo Park, Calif.

In this paper, we shall discuss experimental results obtained using electrostatic probes that were biased to collect saturated ion currents. The probes have been used to determine the freestream charge density and the ionization rise time in the supersonic flows generated by an arc-heated, pressure-driven shock tube. Freestream charge density was measured in the plasma produced by a magnetically driven shock tube. The charge density varied from 10^{10} to 10^{15} electrons/cm^3 and the initial shock tube pressure varied from 0.02 to 1 torr. The measurements of ionization rise time agree with other results at Mach numbers where comparison is possible. A region of Mach numbers not previously covered has also been studied so that complete data on the ionization rise time as a function of Mach number for air now exists for Mach numbers from $M = 8$ to $\approx = 26$. The value of freestream charge density has been inferred from the measured ion currents to cylindrical wires and wedge-shaped electrodes using a theory described below. The agreement between the inferred charge density and the values obtained from microwave interferometers and equilibrium calculations are within a factor of 2. At pressures for which shocks form around the cylindrical wires, making probe interpretation difficult, a new type of probe—a small half-angle wedge—has been calibrated. It is shown that a simple theory can account for the measured results. A more refined theory is required if this probe is to be used without calibration.

Nomenclature

n_∞ = freestream charge density (it is assumed that the electron and ion densities are equal in the freestream)
v_{th} = freestream thermal velocity of ions = $(8kT/\pi M_+)^{1/2}$
η = eV_p/kT
V_p = probe potential
T = ion temperature; when electron temperature > ion temperature use electron temperature
k = Boltzmann constant
M_+ = ion mass
γ = a/r_p
a = sheath radius
r_p = probe radius
S = speed ratio = v_f/v_+
v_f = flow velocity
v_+ = $(2kT/M_+)^{1/2}$
L = probe length
e = charge of positive ion

Introduction

THE measurement of charge density levels and the spatial and temporial variation is important in many areas of plasma physics. The use of electrostatic probes to measure these quantities in supersonic plasma flows is discussed both theoretically and experimentally.

Received March 19, 1969; revision received December 1, 1969. This work was supported by the NASA Langley Research Center and the Bell Telephone Laboratories.

* Program Manager, Electromagnetic Sciences Laboratory. Member AIAA.

† Senior Research Engineer, Electromagnetic Sciences Laboratory.

Theory

A. Free Molecular Cylindrical Probes

When a cylindrical conductor that is small compared to the mean free path is inserted into a plasma, and a voltage large enough to repel all the electrons is applied between the cylinder and another (larger area) electrode in the plasma, the cylinder will collect positive ion current, and a positive ion sheath will form around the probe. In general, the current will be given by an expression of the form

$$I = (n_\infty e v_{th}/4) F(\eta,\gamma,S) 2\pi r_p L \quad (1)$$

1. *Qualitative relationships*

$\gamma \approx 1$

If the sheath is thin the current will be closely approximated by

$$I = (n_\infty e v_{th}/4)(2\pi r_p L) \quad (2)$$

where the first term in parenthesis is the random charge flux density and the second term is the physical area of the probe. If the plasma is flowing, there will be, in addition, a convective term of the form

$$I_c \approx (n_\infty e v_f)(2 r_p L) \quad (3)$$